Semicond. Sci. Technol. **28** (2013) 035002 (7pp) doi:10.1088/0268-1242/28/3/035002

Modeling of photovoltaic cells and arrays based on singular value decomposition

Kun Zhang[1], **Wangkun Jia**[1], **Jack Koplowitz**[1], **Piergiovanni Marzocca**[2] **and Ming-C Cheng**[1]

[1] Department of Electrical and Computer Engineering, Clarkson University, Potsdam, NY 13699-5720, USA
[2] Department of Mechanical and Aeronautical Engineering, Clarkson University, Potsdam, NY 13699-5720, USA

E-mail: mcheng@clarkson.edu

Received 24 September 2012, in final form 19 December 2012
Published 28 January 2013
Online at stacks.iop.org/SST/28/035002

Abstract
An accurate photovoltaic (PV) model is developed based on singular value decomposition (SVD) using measured or simulated data for PV current in terms of cell temperature, solar irradiance and output voltage. The SVD model projects the problem onto a space described by a small number of orthogonal basis functions (or modes). The number of modes adopted for constructing the model is determined based on the magnitudes of the singular values and the desired accuracy. This model is further implemented in a circuit simulator and applied to modeling of a PV array. Two PV test cells are used to verify the validity of the developed model. The SVD model is also demonstrated in a PV array with a non-uniform temperature profile. The developed SVD PV model requires no assumption to construct the model and is remarkably simple and accurate. To our best knowledge, this is the first application of SVD to modeling of semiconductor device characteristics and the first representation of SVD as an electric circuit.

(Some figures may appear in colour only in the online journal)

1. Introduction

Advance of photovoltaic (PV) technology in recent years has made solar energy one of the key alternative energy sources available in the energy market. In order to make the PV energy more affordable, improvement on power efficiency of PV systems has recently been one of the major focuses in the PV research community and industry [1–4]. The efficiency of a PV system not only depends on the cell efficiency and the load but also decreases substantially due to cell mismatch, non-uniform solar irradiance and temperature variation in the PV module/array. To understand and minimize these undesirable effects, a PV cell model that is able to include accurate dependences of both temperature T and solar irradiance E is essential.

The commonly used PV models are based on the equivalent circuit models [5–13]. The model is composed of a photo-current source, one or two parallel diodes, a shunt resistance and a series resistance. Photo-current and series/shunt resistances are influenced by T and E [11–14], and the diode components are strongly dependent on T. However, most of these studies [7–10] do not include the temperature dependence even though many of these parameters are strongly temperature dependent. To include the highly nonlinear T and E dependences on the models for these components, critical assumptions are always needed.

Many methods, including nonlinear fitting [11–13, 15, 16], artificial neural network [17] and genetic algorithms [18], have been reported to evaluate the parameters for the circuit components. To account for the highly nonlinear temperature dependence, more parameters describing thermal influence on each component need to be introduced in the nonlinear model for each component [5, 6, 11]. For example, there are 13 parameters introduced in [11] for the nonlinear components of the circuit model. This requires extensive computation to extract the parameters due to the highly nonlinear characteristics of most components, and often

convergence for the extraction relies on the initial guess of the parameter set.

In this study, an alternative model is presented based on singular value decomposition (SVD) [19–21] to model the output current I_s of a PV cell, accounting for both temperature T and solar irradiance E dependences, influenced by solar cell output voltage V_s. Using the measured or simulated data for I_s in terms of T, E and V_s, SVD projects the problem onto a space described by orthogonal basis functions (modes). The number of modes is chosen according to the magnitude of the singular values and the desired accuracy. It has been shown in this study that the SVD PV model can also be implemented in a circuit simulator, such as Spice. Such capability is useful for the simulation of a PV system together with an electronic system that is always needed to deliver the energy to batteries or power grids. Two test cells are constructed to verify the SVD PV model. Accuracy and simplicity of the developed model are demonstrated in PV cells and a PV array with uniform and non-uniform temperature profiles.

SVD has been applied to many different areas in science, engineering and economics [19–21]. Most applications of SVD for engineering/science problems are centered on signal/image data processing [22–27] and control and linear systems [28–30]. To our best knowledge, this study is the first application of SVD to modeling of PVs and semiconductor devices and the first representation of SVD as an electric circuit. The drawback of the SVD approach is that the SVD PV model does not offer physical insight of PV cells into transport properties, such as diffusion and recombination mechanisms, associated with the model parameters. However, many advantages exist in the SVD approach for such highly nonlinear characteristics, as will be discussed in section 4.

2. SVD photovoltaic model

To construct an SVD model for a PV cell, I_s can be collected from experimental measurements or numerical simulations in terms of V_s, T and E. Based on the current data, a $p \times q$ matrix of current can then be arranged as

$$\mathbf{I_s} = \mathbf{I_s}(T, E, V_s) = \left[\vec{I}_1 \quad \vec{I}_2 \quad \cdots \quad \vec{I}_q\right], \tag{1}$$

where $\vec{I}_j$ ($j = 1$ to q) is the $p \times 1$ current vector of the jth column consisting of current elements measured at p different values of V_s at the jth set of (T, E). In each row (i.e. at a specific value of V_s), the current data are measured at m values of T and n values of E, and thus $q = mn$. In the data set for I_s, uniform increments are taken for V_s, T and E in this study; i.e. $\Delta V_s = V_{s,i+1} - V_{s,i}$, $\Delta T = T_{u+1} - T_u$ and $\Delta E = E_{v+1} - E_v$, where the subscripts $i = 1$ to $(p - 1)$, $u = 1$ to $(m - 1)$ and $v = 1$ to $(n - 1)$.

SVD can be applied to any real matrix as follows:

$$\mathbf{I_s} = \mathbf{U}\Sigma\mathbf{V}^T = \left[\vec{\Phi}_1(V_s) \quad \vec{\Phi}_2(V_s) \quad \cdots \quad \vec{\Phi}_p(V_s)\right]\mathbf{A}(T, E), \tag{2}$$

where $\mathbf{U}$ and $\mathbf{V}$ are $p \times p$ and $q \times q$ unitary matrices ($\mathbf{U^TU} = \mathbf{I}$ and $\mathbf{V^TV} = \mathbf{I}$), respectively, and Σ is a $p \times q$ diagonal matrix with the non-zero elements known as the singular values.

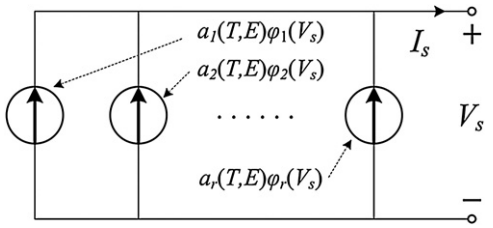

Figure 1. Circuit representation of the SVD model for a PV cell.

The $p \times 1$ vectors $\vec{\Phi}_k$ ($k = 1$ to p) are the columns of $\mathbf{U}$ (the basis functions or the modes in the V_s space), and they are orthogonal to each other. The singular values σ_k (or the diagonal elements of Σ) are arranged in decreasing order, i.e. $\sigma_1 \geqslant \sigma_2 \geqslant \cdots \geqslant \sigma_l$, where $l = \min(p,q)$. Each column $\vec{I}_j$ of $\mathbf{I_s}$ can be expressed as the linear combination of $\vec{\Phi}_k$ in a function space $\boldsymbol{S}$, and $\vec{I}_j$ corresponds to a condition given by a set of T–E values associated with the jth column of $\mathbf{A}$. In general, σ_k decreases rapidly. If σ_k is negligible for $k > r$ ($1 \leqslant r < l$), only the first r basis functions ($\vec{\Phi}_1, \ldots, \vec{\Phi}_r$) are needed to describe the current. Thus, in (2) only the first r columns of $\mathbf{U}$ and the first r rows of $\mathbf{A}$ are included in calculations. A low-rank approximation for the element of the current matrix $\mathbf{I}_s$ is then expressed as

$$I_{s,ij} = \sum_{k=1}^{r} a_k[(T, E)_j]\varphi_k(V_{s,i}), \tag{3}$$

where $\varphi_k(V_{s,i})$ is the ith element of the basis function $\vec{\Phi}_k$, and $a_k[(T,E)_j]$ is the kth element of the jth column of the 'reduced' $r \times q$ matrix $\mathbf{A}$. For brevity, the indices, i and j, in (3) are dropped and the output current is expressed in terms of T, E and V_s as

$$I_s(T, E, V_s) = \sum_{k=1}^{r} a_k(T, E)\varphi_k(V_s). \tag{4}$$

As shown in figure 1, the contribution from each mode can be represented by a dependent current source with a value of $a_k\varphi_k$ in the function space $\boldsymbol{S}$, where a_k is determined by T and E, and φ_k is a function of V_s. Based on (4), the dependent circuit sources given in figure 1 can be implemented in a circuit simulator and solar cell modules/arrays can be constructed, together with bypass and blocking diodes and appropriate load impedance, for the simulation of the PV systems. In the simulations presented in the next section, linear interpolation is applied in LTSpice to estimate the value between two discrete values. Usually, σ_k decreases rapidly as k increases; meaning $r \ll p$ and $r \ll q$. The total number of data needed for the SVD model given in (4) is equal to $(p + q)r$ that is thus significantly smaller than the original data size of pq.

3. Applications

In this study, two different test PV cells are used to collect data for the PV currents that are applied to construct two different SVD models and to examine the influences of operating temperature/irradiance and data fluctuations on the SVD models. One PV cell structure is constructed in a device simulator PC1D [31] and the other is defined by a conventional

two-diode circuit model [11]. These two test cells are used to demonstrate the accuracy and effectiveness of the SVD approach for two PV cells with very different characteristics. Because the device simulator cannot perform simulation of a PV array, the test cell based on the two-diode model is included to allow us to demonstrate the capability of the SVD approach for the simulation of a PV array with uniform and non-uniform temperature profiles. These two test PV cells and how their data are collected are briefly described below. In this study, 1 sun is defined as 0.1 W cm^{-2} at the AM1.5 spectrum, and simulations of the SVD model and two-diode circuit are all carried out in LTSpice [32].

Device simulator. Characteristics of PV cells in the PC1D [31] are determined by transport parameters of electrons and holes, which are derived from numerical solutions of electron/hole continuity and current equations coupled with the Poisson equation. The simulator provides spatial distributions of the electron/hole concentrations and current densities and electrostatic potential in a cell as functions of the applied voltage, solar irradiance and temperature. Using PC1D, simulations of a crystalline Si PV cell are performed to collect the current data given in (1) at voltage V_s ranging from 0 to 0.75 V with a step of 0.01V (i.e. $p = 76$). The geometry and physical and material parameters are the same as those of the solar cell example included in the PC1D software package. Two different sets of data are used to construct the SVD models. Case 1 includes temperature T varying from 10 to 70 °C with an increment of 10 °C (i.e. $m = 7$), and case 2 from −20 to 100 °C with the same increment (i.e. $m = 13$). For both cases, solar irradiance E varies from 0 to 1.2 sun with a step of 0.4 sun (i.e. $n = 4$). This leads to 28 or 52 conditions of (E, T) for each V_s in case 1 or case 2, respectively.

Two-diode circuit model. Output current for the two-diode model is given as

$$I_s = I_{ph} - I_{s1}(e^{eV_d/n_1kT} - 1) - I_{s2}(e^{eV_d/n_2kT} - 1) - \frac{V_d}{R_{sh}}, \quad (5)$$

where I_{ph} is the photocurrent, R_s is series resistance, R_{sh} is shunt resistance, I_{s1} is saturation diffusion current, I_{s2} is saturation recombination current and n_1 and n_2 are ideality factors. The diode voltage $V_d = V_s + I_sR_s$. In [11], $n_1 = 1$ and other model parameters are expressed as

$$I_{s1} = K_2T^3e^{K_3/T},$$

$$I_{s2} = K_4T^{3/2}e^{K_5/T},$$

$$I_{ph} = K_0E(1 + K_1T),$$

$$n_2 = K_6 + K_7T,$$

$$R_{sh} = K_{11}e^{K_{12}T},$$

$$R_s = K_8 + \frac{K_9}{E} + K_{10}T,$$

where the values of K_1 to K_{13} used in this study are listed in table 1. Using this parameter set, Spice simulations are carried out to collect the data for the current matrix in (1). In this data collection, V_s ranges from −0.1 to 0.65 V with $\Delta V_s = 0.01$ V ($p = 76$), T varies from 10 to 70 °C with $\Delta T = 10$ °C ($m = 7$) and E varies from 0.1 to 1.3 sun with $\Delta E = 0.4$ sun (i.e. $n = 4$). This leads to 28 conditions of (E, T) for each V_s. It should be mentioned that the model for R_s adopted from [11] includes the E dependence as $1/E$, which induces a singularity at very small solar irradiance and does not offer reasonable description at a small value of E. The collected data thus only cover E as small as 0.1 sun. This is however not a concern in this study. This work demonstrates that the SVD modes generated from a data set obtained from different PV cells can accurately reproduce the characteristics of the PV cells used to generate the data.

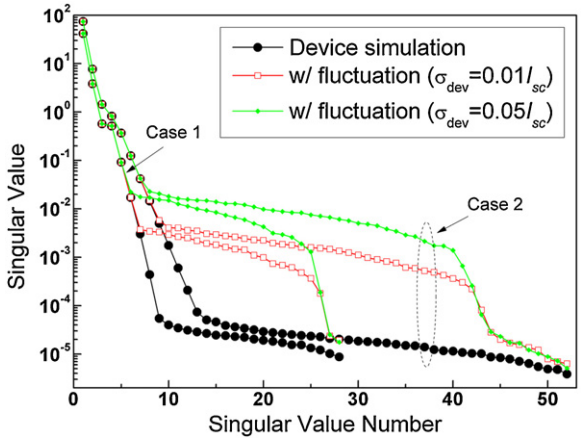

Figure 2. Singular values for data generated from device simulations including case 1 and case 2. The singular values for the data with added fluctuations are also included. σ_{dev} is the standard deviation.

Table 1. Selected parameter values in the two-diode circuit model.

$K_0 = 0.27$ (V^{-1})	$K_7 = 0$
$K_1 = 6.8 \times 10^{-4}$ (K^{-1})	$K_8 = 2$ (Ω cm^2)
$K_2 = 0.225$ (K^{-3} A cm^{-2})	$K_9 = 1.13 \times 10^{-2}$ (V^2)
$K_3 = -1.26 \times 10^4$ (K)	$K_{10} = -4.47 \times 10^{-3}$ (Ω cm^2 K^{-1})
$K_4 = 0.118$ (K$^{-3/2}$ A cm^{-2})	$K_{11} = 2.3 \times 10^6$ (Ω cm^2)
$K_5 = -7.32 \times 10^3$ (K)	$K_{12} = -2.4 \times 10^{-2}$ (K^{-1})
$K_6 = 2$	$n_1 = 1$

Although equal divisions are taken for E, T and V_s in this study for simplicity, the decomposition can be performed on matrices of data with unequal divisions. Since I_s is highly nonlinearly dependent on V_s and T, a higher number of divisions are chosen in voltage and temperature to improve the accuracy. I_s however approximately linearly depends on solar irradiance, and thus only four divisions are used to cover all the irradiance range.

3.1. SVD model using data derived from PC1D

Data generated from device simulations using PC1D are used to perform SVD, as described in section 2. The singular values σ_k, displayed in figure 2 for both cases, decrease rapidly. Because of a smaller range of operating temperature used in case 1, its σ_k decrease faster than those of case 2. For example, σ_1/σ_5 is near 450 or 230 for case 1 or case 2, respectively. To achieve a similar accuracy, the SVD model for the wider operating conditions, therefore, needs more modes than that for

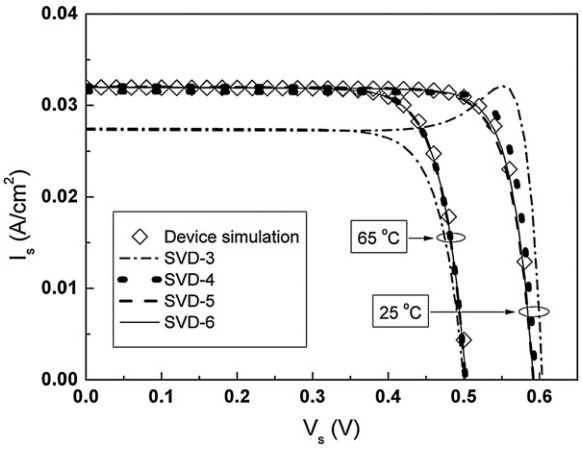

Figure 3. *I–V* characteristics of the PV cell derived from device simulation and the SVD model of case 1 at 25 and 65 °C. Different numbers of modes are used in the SVD model. Solar irradiance is 1 sun.

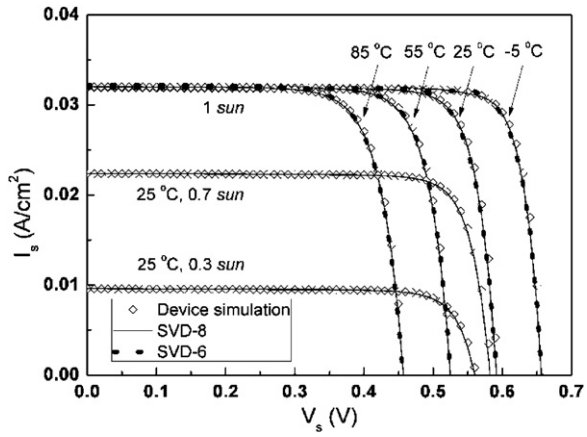

Figure 4. *I–V* characteristics of the PV cell derived from device simulation and the SVD model of case 2 at different temperatures and irradiances, wherein SVD results are obtained using six modes and eight modes.

narrower operating conditions. This will be further observed below. Figure 2 also displays a standard feature of σ_k whose curve suddenly becomes flattened when σ_k is very small. It is believed that this results from the small numerical fluctuation of the collected data that make the magnitudes of the smaller σ_k less distinguishable. To illustrate this phenomenon, we generated two additional sets of data for $\mathbf{I_s}$ from the collected data by adding random Gaussian fluctuations with standard deviations σ_{dev} of $0.01I_{\text{sc}}$ and $0.05I_{\text{sc}}$, where I_{sc} is the short circuit current of the PV cell. The results show that, before the curve with larger fluctuations becomes flattened, its singular values are nearly identical to those with smaller fluctuations. This gives the following implication. If the fluctuations inherited in the measured data are not too large and the σ_k curve starts becoming flattened at a large singular value number k such that $r < k$ (where r is the number of modes needed to reach the desired accuracy), the low-rank SVD model is able to capture the essential characteristics without being influenced by the random fluctuations.

To demonstrate the accuracy of the SVD approach, simulation results from the SVD PV models for cases 1 and 2 are compared, as shown in figures 3 and 4, respectively, to those derived from PC1D device simulations under the (*T,E*) conditions, different from those used for the extraction of σ_k and φ_k. Figure 3 shows the case 1 results at 25 and 65 °C, where the accuracy of the SVD model is illustrated using different numbers of modes at both operating temperatures. In case 1, σ_4 is quite close to σ_3 (see figure 2), indicating that the fourth mode cannot be neglected as illustrated in figure 3. With the fourth mode included, the SVD model (SVD-4) is able to accurately describe the *I–V* curve at 65 °C, and inclusion of the fifth or higher-number modes at 65 °C results in negligible improvement. While at 25 °C, evident deviation from the device simulation including the first four modes is still observed near the maximum power point where the I_s–V_s relation becomes highly nonlinear. In this case, six modes are required at 25 °C to reach a similar accuracy using four modes at 65 °C. This suggests that the SVD model for the PV cell requires a larger number of modes to reach a reasonable accuracy at lower temperature than at higher temperature. The modes associated with larger singular value numbers (such as the fifth and sixth modes in this case), although offering little influence on the PV characteristics at higher temperature, may provide critical information needed to capture the highly nonlinear *I–V* characteristics at lower temperature.

Because σ_k decreases more slowly as k increases in case 2, as shown in figure 2, a larger number of modes are needed to accurately describe the *I–V* curves in case 2 than in case 1. As illustrated in figure 4, although the SVD model with six modes offers very good results at 1 sun, small deviation of the SVD model from the device simulations is still observed at 25 and −5 °C near their maximum power points. To achieve a similar accuracy to case 1 presented in figure 3, eight modes are needed at 25 and −5 °C in case 2, as shown in figure 4. Excellent agreement between the eight-mode SVD PV model and device simulations at 25 °C for irradiance less than 1 sun is also observed in figure 4.

3.2. SVD model using data derived from the two-diode circuit model

The singular values σ_k from SVD on the current data obtained from the test PV cell represented by the two-diode circuit model are illustrated in figure 5. This dataset actually gives rise to a faster decrease in the singular values than those presented in figure 2. For example, σ_1/σ_5 is near 570 in figure 5 compared to 450 or 230 (case 1 or 2) in figure 2. This suggests that the SVD model constructed based on the two-diode circuit model with a smaller number of modes should be able to reach the same accuracy to the one built using PC1D with a larger number of modes. Similar to figure 2, figure 5 also shows that data with added Gaussian fluctuations result in a flattened singular value curve at a smaller singular value number. In addition, before the curve with larger fluctuations becomes flattened, its singular values are nearly identical to those with lower fluctuations.

Demonstration of accuracy for this SVD model is illustrated in figures 6 and 7. With only four modes, the

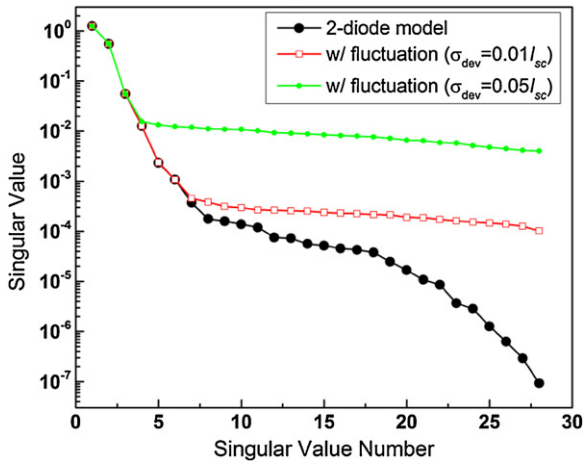

Figure 5. Singular values for data generated from the two-diode circuit model. Singular values for the data with added fluctuations are also included.

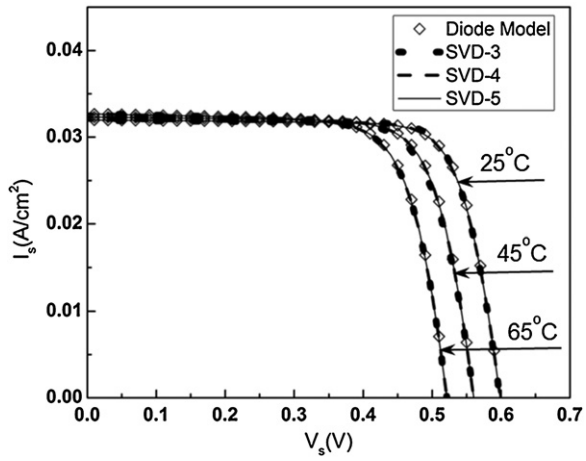

Figure 6. *I–V* characteristics of the PV cell derived from the two-diode circuit model at 25 , 45 and 65 °C and 1 sun. Different numbers of modes are used in the SVD model.

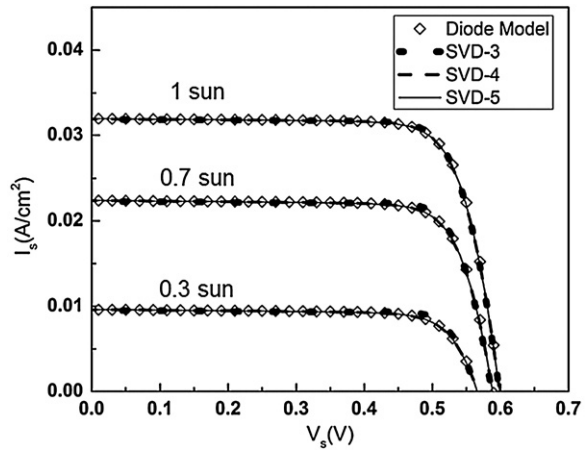

Figure 7. *I–V* characteristics of the PV cell derived from the two-diode circuit model and the SVD models at 25 °C and different solar irradiances. Different numbers of modes are used in the SVD model.

SVD model generated from the two-diode circuit yields nearly the same *I–V* curves generated from the two-diode

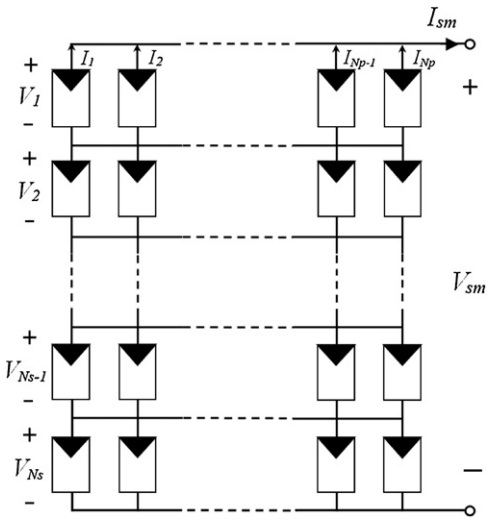

Figure 8. A PV module using a total cross-tied configuration with N_s series and N_p parallel cells.

circuit for temperature ranging from 25 to 65 °C at various solar irradiances within the range used to perform the decomposition. Four-mode and five-mode SVD models lead to essentially identical results. In addition, one feature is worthwhile to mention. In figure 3, the three-mode SVD model derived from PC1D for case 1 provides *I–V* characteristics that are substantially different from those derived from the four-mode model. On the other hand, small difference is observed in figures 6 and 7 between the three-mode and four-mode models. This can be easily understood from the singular values displayed in figures 2 and 5 for these two different test PV cells. In figure 5, σ_4 is considerably smaller than σ_3, which indicates that the inclusion of the fourth mode will just slightly improve the SVD model for the two-diode PV cell. In fact, three modes are able to offer high accuracy for this test cell. However, σ_4 in figure 2 is only slightly smaller than σ_3, which implies that the third and fourth modes are equally important in the SVD model constructed from PC1D. This is clearly illustrated in figure 3 where results derived from the first three modes deviate substantially from the curves obtained from PC1D.

The SVD PV model derived from the PV test cell represented by the two-diode model is further applied to construct a PV module with a 6 × 6 array configuration. A total cross-tied configuration shown in figure 8 is selected in this study because, according to the study in [17], this configuration offers superior performance under partially shaded conditions compared to any other configuration. Figure 9 presents the *I–V* characteristics of a 6 × 6 module constructed from the two-diode circuit model given in (5) and the SVD model in (4) including uniform and non-uniform temperature profiles over the module. In figure 9, a 25 cm^2 area is used for each cell of the module, and the output current is presented in A instead of A cm^{-2} as in other figures. Although the assumption of a fixed non-uniform temperature profile for different operating currents and voltages may not be realistic, it is just a setup to examine the accuracy and robustness of the SVD model under a non-uniform/mismatched condition. Excellent agreement between the SVD model and the two-diode circuit model is observed for the uniform case at different

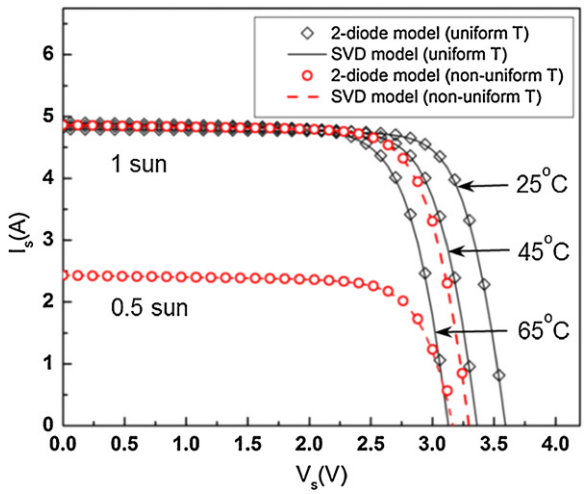

Figure 9. *I–V* characteristics of a 6 × 6 PV module constructed using the two-diode circuit model and the four-mode SVD model. For the curves with non-uniform temperature, a hot-spot is localized near the center of the module. A peak temperature of 75 °C is assigned to a cell near the center of the array, and cell temperature decreases by 10 °C consecutively in the adjoining cells until temperature reaches 45 °C.

temperatures and for the case with a non-uniform temperature profile at different solar irradiances.

4. Discussions

Accuracy and simplicity of the SVD approach have been demonstrated using two very different test PV cells in this work for wide operating conditions of solar irradiance, temperature and voltage, including a module of a 6 × 6 configuration with uniform and non-uniform temperature profiles. Construction of the SVD model is merely a matrix decomposition and is extremely simple. There are many SVD subroutines available online in different languages [33] that can perform such a simple decomposition. In Matlab, a single command is also available to carry out this. Once the current matrix $\mathbf{I_s}$ is arranged in the format given in (1), execution of the command *svd* in Matlab returns the matrices $\mathbf{U}$, Σ and $\mathbf{V}$ that give the basis functions $\vec{\Phi}_k$, the matrix $\mathbf{A}$ and singular values σ_k, as presented in (2)–(4). The SVD model with φ_k and a_k given in (4) is then ready to be implemented in a Spice simulator or other simulation languages and platforms.

Construction of the highly nonlinear and implicit diode circuit model given in (5) on the other hand is nontrivial. The procedure involves two steps: (i) determination of model expressions for parameters $I_{\rm ph}$, I_{s1}, I_{s2}, n_1, n_2, R_s and $R_{\rm sh}$ in (5), and (ii) extraction of the coefficients introduced in these expressions. The parameters are nonlinearly dependent on E and T, and their expressions as functions of E and T cannot be easily defined. Some expressions are derived from device physics with some fitting coefficients and some just assumed to be polynomial and/or rational functions of E and/or T. These assumptions always impose limits on the model that may lead to errors in some operating conditions. For example, both R_s and $R_{\rm sh}$ have been shown [14] to be dependent on solar irradiance. $R_{\rm sh}$ is however assumed to be independent of E in [11]. Also, the dependence of R_s on E in [11] is specified as $1/E$ that is not valid at small solar irradiance. A different expression will be needed for operation at small solar irradiance. It is common to find very different expressions for the same parameter in different pieces of literature [11, 13].

As to the second step, accurate extraction of the coefficients introduced in these nonlinear expressions for the model parameters in the diode circuit model requires significant computational effort and usually relies on numerical optimization algorithms [11, 15, 16] (such as particle swarm optimization [16, 34], the Levenberg–Marquardt least-squares method [11, 35, 36] or other nonlinear least-squares methods) together with iteration techniques. Unlike the SVD approach, initial guess for all the coefficients are needed and computational time and convergence depend on the choice of the initial set of coefficients. Implementation of these methods to determine the coefficients/parameters and to construct the two-diode model is considerably more complicated and time-consuming than the SVD approach.

There are many advantages in the conventional diode model. For example, the built-in diode model is available in any Spice tool and many other electronic circuit simulators, and the major device parameters are relevant to physical transport properties of charge carriers in PV cells. The developed SVD model however provides an alternative for modeling of PV cells and systems. This alternative offers its simplicity for constructing the PV model and its accuracy for prediction of the cell and array characteristics. One of the great advantages of the SVD approach is that the model does not need any assumption and can be used to construct any complicated nonlinear characteristics for any operating range as long as the data set used to construct the model covers the range of interest. Moreover, for a PV cell fabricated using a new structure with new materials, an accurate SVD PV model can be built without difficulty even before the physics of the new cell structure is well understood. This study also presents a new application of SVD to modeling of physical characteristics of a device, which is not a conventional application for SVD. However, it needs to be pointed out that the SVD model is not presented in this study to displace or challenge the conventional diode model. As discussed above, each model exhibits its own pros and cons. The SVD model may be able to provide a simple approach to accurately model the PV characteristics but offers no insight into the physics of PV characteristics and material parameters. On the other hand, the conventional physics-based diode model provides clear concepts about how device physics and material parameters influence the PV performance.

5. Concluding remarks

SVD has been applied on the data of the solar cell current as a function of cell temperature, solar irradiance and PV output voltage to extract the basis functions and their singular values. The physical characteristics of the PV cell are then projected onto a small number of the basis functions (or modes). The number of the modes needed to describe the characteristics is determined by the singular values and the desired accuracy. Study of the singular values from the collected data and the

number of modes adopted to construct an accurate SVD model show that the singular values of a data set with a smaller temperature range diminish faster than that with a large range of operating temperature. Therefore, more modes are needed for a larger temperature range to achieve a similar accuracy. In addition, more modes are required to accurately capture the *I–V* characteristics in the highly nonlinear region at lower operating temperature than at higher temperature.

The SVD model has been implemented in a circuit simulator to perform simulations of single PV cells and a PV array. Unlike the conventional PV diode circuit model, construction of the SVD model is extremely simple. The SVD approach has been demonstrated with high accuracy in single cells and array structures. It has also been shown that the model of a PV array constructed using the SVD approach is able to accurately account for effects of a non-uniform temperature profile with a high peak temperature.

Acknowledgment

This work was in part supported by the Army Research Office under grant W911NF-05-1-0339.

References

[1] Donne A L, Acciarri M, Narducci D, Marchionna S and Binetti S 2009 *Prog. Photovolt., Res. Appl.* **17** 519–25
[2] Green M A and Ho-Baillie A 2010 *Prog. Photovolt., Res. Appl.* **18** 42–47
[3] Fan Q H *et al* 2010 *Sol. Energy Mater. Sol. Cells* **94** 1300–2
[4] Green M A, Emery K, Hishikawa Y and Warta W 2010 *Prog. Photovolt., Res. Appl.* **18** 144–50
[5] Maffezzoni P and D'Amore D 2009 *IEEE Trans. Circuits and Syst. II* **56** 162–6
[6] Asif S and Li Y 2008 *J. Propulsion Power* **24** 1018–22
[7] Shvets E Y, Khrypko S L and Zubko E I 2009 *Radioelectron. Commun. Syst.* **52** 16–23
[8] Ortiz-Conde A, Sanchez F G and Muci J 2006 *Sol. Energy Mater. Sol. Cells* **90** 352–61
[9] Ouennoughi Z and Chegaar M 1999 *Solid-State Electron.* **43** 1985–8
[10] Munji M K, Okullo W, Dyk E E and Vorster F J 2010 *Sol. Energy Mater. Sol. Cells* **94** 2129–36
[11] Gow J A and Manning C D 1999 *IEE Proc. Electric Power Appl.* **146** 193–200
[12] Haouari-Merbah M, Belhamel M, Tobias I and Ruiz J M 2005 *Sol. Energy Mater. Sol. Cells* **87** 225–33
[13] Burgers A R, Eikelboon J A, Schonecker A and Sinke W C 1996 *Proc. 25th IEEE Photovoltaic Specialists Conf. (Washington, DC)* pp 569–72
[14] Sharma A K, Dwivedi R and Srivastava S K 1991 *IEE Proc. G Circuits Devices Syst.* **138** 301–6
[15] Easwarakhanthan T, Bottin J, Bouhouch I and Boutrit C 1986 *Int. J. Sol. Energy* **4** 1–12
[16] Sandrolini L, Artioli M and Reggiani U 2010 *Appl. Energy* **87** 442–51
[17] Karatepe E, Boztepe M and Colak M 2007 *Sol. Energy* **81** 977–92
[18] Jervase J A, Bourdoucen H and Al-Lawati A 2001 *Meas. Sci. Technol.* **12** 1922–5
[19] Bretherton C S, Smith C and Wallace J M 1992 *J. Clim.* **5** 541–60
[20] Nardone C 1991 *Plasma Phys. Control. Fusion* **34** 1447–65
[21] Bekiros S D 2009 *Econ. Lett.* **103** 36–38
[22] Narwaria M and Lin W 2012 *IEEE Trans. Syst. Man Cybern. B* **42** 347–64
[23] Jiang Y, Tang B, Qin Y and Liu W 2011 *Renew. Energy* **36** 2146–53
[24] Zhao X and Ye B 2009 *Mech. Syst. Signal Process.* **23** 1062–75
[25] Costantini R, Sbaiz L and Susstrunk S 2008 *IEEE Trans. Image Process.* **17** 42–52
[26] Deng T B and Nakagawa Y 2004 *IEEE Trans. Signal Process.* **52** 2513–27
[27] Stoica P, Selen Y, Sandgren N and Van Huffel S 2004 *IEEE Trans. Biomed. Eng.* **51** 1568–78
[28] Klema V C and Laub A J 1980 *IEEE Trans. Autom. Control* **25** 164–76
[29] Rojas O J, Goodwin G C, Serón M M and Feuer A 2004 *Int. J. Robust Nonlinear Control* **14** 1207–26
[30] Hojabri H, Mokhtari H and Chang L 2011 *IEEE Trans. Ind. Electron.* **58** 949–59
[31] http://www.pv.unsw.edu.au/links/products/pc1d.asp
[32] http://www.linear.com/designtools/software/
[33] See a list of libraries at http://en.wikipedia.org/wiki/Singular_value_decomposition
[34] Kennedy J 1997 *Proc. IEEE Int. Conf. on Evolutionary Computation* pp 303–8
[35] Levenberg K 1944 *Q. Appl. Math.* **2** 164–8
[36] Marquardt D 1963 *J. Soc. Appl. Math.* **11** 431–41